A QUICK TECHNIQUE OF FLOOD DETECTION AND MAPPING BASED ON LAND COVER/LAND USE CHANGES (CASE STUDY: THE 2022 FLOOD EVENT OF TALEGHAN CITY OF IRAN)

M. Gheysouri[1], Sh. Khalighi Sigaroodi*[2], M. Kalehhouei[3], A. R. Moghadamnia[2]

[1] Ph.D. student, Watershed Management, Faculty of Natural Resources, University of Tehran, Iran, Email: m.gheysouri@ut.ac.ir

[2] Department of Watershed Management Engineering, Faculty of Natural Resources, University of Tehran, Karaj, Iran, Email: khalighi@ut.ac.ir and a.moghaddamnia@ut.ac.ir

[3] Ph.D. student, Watershed Management, Faculty of Natural Resources, Tarbiat Modares University (TMU), Nour, Mazandaran, Iran, Email: k.mahin@modares.ac.ir

Commission IV, WG IV/3

KEY WORDS: Instant management, Google Earth Engine, Land cover, Sentinel, Stream, Three hours.

ABSTRACT:

Flood as one of the most devastating natural disasters, causes significant tangible and intangible damages to watershed residents each year. When flood occurs, changes in land use (LU) and land cover (LC) relative to climate change and other edaphic factors have remarkable impacts on flood generation. Furthermore, application of complicated models with various inputs is costly and time-consuming. In this study, with the aim of determining the parameters affecting the recent floods in the Taleghan watershed, first, maps of the flooded areas and changes in LU and LC was extracted using' Sentinel 1 & 2 by coding the Google Earth Engine. In the extraction of LU, seasonal composites were used and the winter season was eliminated. Next, using the override command in the ARCGIS 10.8.1 software, the extracted maps were combined and evaluated. The results show that the use of urban and forest lands was limited to the lands next to the rivers and streams, which are the places where the floods pass, and this factor has increased exposure to flood. According to the composition of the maps in the Taleghan watershed, floods occurred in areas where there was no LC and the flooded areas we are located in the upper part of villages where natural LC was lost as a result of livestock grazing or human manipulation. It can be concluded that the use of simple models and basic maps can help experts identify flood zones.

* Corresponding author

https://doi.org/10.5194/isprs-annals-X-4-W1-2022-229-2023

1- Introduction

In recent years, climate change has significantly increased the risk of natural hazards globally and is seen as a main threat to ecosystems and humans (Song and Liang, 2022). Most of these hazards are climate-related and seriously endanger the livelihoods and food security of millions of people (Parven et al., 2022). Besides natural hazards, climate change and LU caused by human activities can also increase environmental risks by reducing the providing of ecosystem services to humans (Song and Liang, 2022). Human activity and associated carbon emissions are major drivers of land use and climate change, with significant impacts on extreme events such as flooding (Pal et al., 2022), and this can affect the dynamics of the hydrological cycle and the interactions between infiltration and runoff (Carvalho et al., 2022). These changes are an essential characteristic of runoff processes that affect erosion, infiltration and evapotranspiration (Tilahun, 2015). As it is widely recognized that LULC is one of the most important factors affecting watershed hydrologic response and flood occurrence (Rigby et al., 2022). Floods are one of the most devastating natural disasters, causing enormous damage to property, infrastructure and human life. Total economic losses from floods since the end of the 20th century have been estimated at $386 billion (Wang et al., 2011). Between 1995 and 2015, 47% of natural disasters were flood-related, directly affecting 2.3 billion people, and most of them live in Southeast Asia (Wahlstrom and Guha-Sapir, 2015). Intensification of the hydrological cycle after global warming could increase water-related risks such as flooding (Khadka et al., 2020). As a result, there is concern about the danger to people and property from flooding (Alfieri et al., 2017). Depending on the material presented, flooding is a dynamic process driven by the complex interplay of watershed management, meteorological, hydrological and geomorphological conditions. It is a complex, nonlinear process that cannot be effectively controlled by a simple linear process (Talbot et al., 2018). A lot of research has been done on the effects of LU and flooding, including Rahman et al. (2021) investigated the relationships between LC change, relative changes in population growth, road density, and flood from 2000 to 2017. The results show that the highly flood sensitive areas increased by 19.72% in the years studied and the population growth rate increased by 51.68% over the same period. Vulnerability to precipitation and flooding, according to LULC projections, Pal et al. (2022) showed that maximum monthly precipitation increases by about 40–50 mm by 2100, while the change in agricultural and residential areas is about 0.071 million km^2. Areas affected by severe flooding will now increase by 122% (0.15 m km^2) due to land use change. Li and Bortolot (2022), object-oriented image classification was used to assess the impact of impervious land cover on peak flood rate and total volume, they showed that impervious areas under the effects of urban redevelopment have increased by 32% from 1950 to 2018. Land cover impermeability increased storm peak and volume by up to 57.5% and 75.3%, respectively. Purswani et al. (2022) examined land cover change at different spatial and temporal scales to understand its potential impacts on the environmental impacts in the Gandhinagar district of Gujarat, India, and found that rapid growth in rural and urban areas was showed that it was mainly accompanied by a reduction in shrubland. According to the content mentioned, the change in land cover becomes a factor disrupting the ecological balance of the ecosystem, which ultimately causes floods. As a result, the ecological risk of land cover change is still a new concept compared to established natural disaster risk assessment frameworks (Song and Liang, 2022). Additionally, urbanization is on the rise universally and is the foremost basic cause of worldwide land-use change (Purswani et al., 2022). This requires analysis of land cover and land use change at different spatial and temporal scales to understand its potential environmental impacts. In addition, urban drainage systems have historically been designed to mitigate specific floods that recur at regular intervals. However, increased the impervious cover of the land due to urban regeneration has increased the imperviousness of the surface, which causes human and financial losses with the increased peak discharge and flood levels (Li and Bortolot, 2022).

In this study, Taleghan watershed was chosen as case study that is one of the most flood-prone watersheds in Iran. Due to its unique geographical location, climatic characteristics, topography, landscapes, geomorphological and geological sites, and tourist attractions and exposure to floods. The main purpose of this study is to determine the effective factors in occurring floods and detection of flooded areas based on land cover and land use change using Sentinel 1 & 2 by coding the Google Earth Engine. The proposed technique is quick with the shortest possible time. As a part of this study, the flood occurred in the July 29, 2022 in the Taleghan watershed was evaluated to determine the effective factors. All the factors mentioned were extracted and assessed within 3 hours, which can help managers in flood risk management as a cost-effective and quick technique.

2- Materials and methods

2-1- Introduction of case study

The Taleghan watershed is located 120 km northwest of Teheran, with an area of 1243.03 km^2 and an average height of 2548 m above sea level (Figure 1). A particular feature of this basin is its high altitude and steep slope. Therefore, its minimum height is equal to 1262 m and its maximum height is 4373 m. The long-term average temperature and precipitation of the Taleghan is 24 °c and 448 mm, respectively.

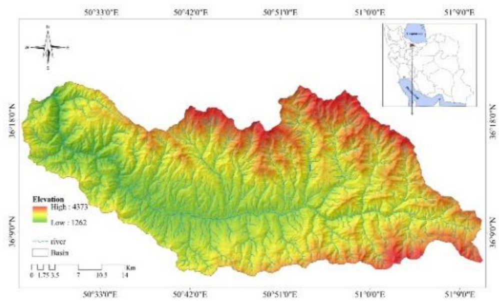

Figure 1. Location of the Taleghan watershed in Iran

2-2- Research method

Due to its special geological structure and the existence of human manipulations and many mines, the Taleghan watershed is exposed to massive floods every year, which causes a lot of human and financial losses. Consequently, the identification of effective factors in the formation of floods is one of the solutions for dealing with floods and managing flood-prone areas. In current study, to determine the effective parameters on floods, using Sentinel 1&2, and coding in the Google Earth Engine, flood, NDVI and LU index for 2022 of Taleghan watershed were extracted. From the Arcmap environment, the area of each user and its distribution in the study area were extracted.

Satellite Data

For this study, the Sentinel 1&2 time series data to map LULC classes. Sentinel 2 provides high temporal resolution data with rich spectral patterns, including 13 spectral bands. Six terrestrial surveillance bands, comparable to Landsat 8 (red: 665 nm, blue: 490 nm, green: 560 nm, NIR: 842 nm, SWIR1: 1910 nm, and SWIR2: 2190 nm) and three additional bands covering the red - edge part of the spectrum which are centered at 705 nm, 740 nm, and 783 nm, and a NIR narrow band at 865 nm (https://sentinel.esa.int/ web / sentinel / missions / sentinel 2).

Flood zoning extraction

In this study, unlike the usual methods of extracting flood-prone areas, flood-prone areas were separated by coding in the Google Earth Engine environment with the help of the Sentinel 1 sensor with a spatial resolution of 10 m. In this method, by combining two images before and after the flood, the flood-prone areas were separated and by classification in the ArcMap, the flood-prone areas were divided from the flood-free areas.

Normalized difference vegetation index (NDVI)

The Normalized Difference Vegetation Index (NDVI) is a simple graphical indicator commonly used to analyze RS measurements and assess whether observed targets contain healthy green vegetation. NDVI quantifies vegetation by measuring the difference between near-infrared (NIR) (vegetation is highly reflective) and red light (vegetation is absorbed/reflects less) (equation 1). NDVI values range from +1 to -1, where -1 is typically water and +1 is typically dense, lush vegetation. Therefore, NDVI can be supposed to be an indicator of healthy green vegetation. Formally, NDVI is given by Braun and Herold (2004) as Eq. (1).

$$NDVI= (NIR-VIS)/ (NIR+VIS) \quad (1)$$

Where VIS and NIR = stand for the spectral reflectance measurements acquired in the visible red and near-infrared locales, respectively.

Land use change extraction

First, all images with cloud cover lower than 30% have been filtered first. Afterwards, the S2cloudless algorithm was used in S 2 to suppress clouds, snow and noise in the images. In the next step of extracting time-spectrum references, two methods were considered to achieve the research goal; 1: Seasonal synthesis method: We used the median reducer to generate synthetic imagery for cloudless seasons (Tsai et al., 2018). In this method, the NDVI index was first separated using satellite images of three seasons: spring (March, April, and May), summer (June, July, and August) and autumn (September, November, and December). Winter images were excluded due to high clouds and snow cover. This approach was developed to include phonological information in LULC classification (Xu et al., 2016).
To the spectral bands, the following spectral indices were calculated: normalized difference built - up index (NDBI; (Kulkarni et al., 2021), and green normalized difference vegetation index (GNDVI; (Gitelson et al., 1998)). In the final stage, five land uses (barren, agricultural, forest, urban, and water) were analyzed using allocated educational points.

3- Results

3-1- Study on changes in LU

In this study, LU changes for 2022 were identified (kappa coefficient= 0.87 & overall accuracy= 0.89). The percentage of the area of each land uses in the region in 2022 for barren LU, agricultural land, forest and garden land, urban land and water is 93.9%, 1.65%, 20.2% and 1.1% respectively. According to Figure 2, in the current area, majority of the surface of the area is barren land, and only a very small part of the case study consists of forest and agricultural land.

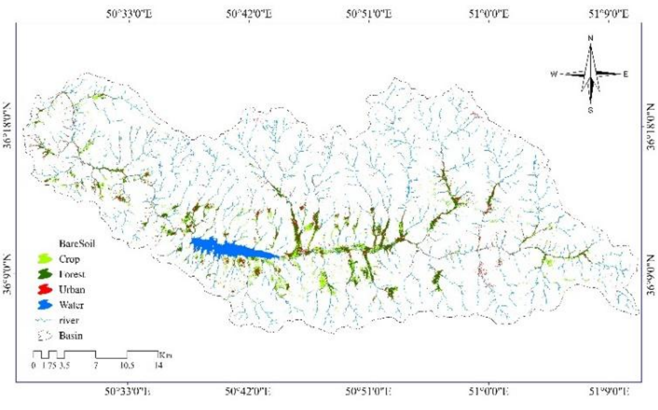

Figure 2. LULC maps of the study area resulting from: (a) S-2 seasonal composites

3-2- Floodplains

In this study, the Sentinel 1 sensor image products were used to study the role of factors affecting summer flooding in the Taleghan watershed. A flood map with a spatial resolution of 10 m was obtained from the study area (Figure 3). About 11.5% of the 1243 km^2 study area is affected by flooding, which mainly includes areas close to rural areas.

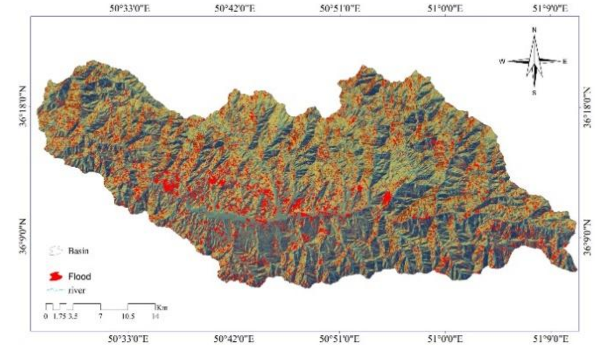

Figure 3. Flood zone in the study area

3-3- Extraction of LC changes

Considering that the studied area has a low mass cover or many forest lands in the form of semi-arid and dense pastures, and it is not possible to distinguish and identify them on the images for the user. As a result, the NDVI was extracted for the month of July to August 2022 (Figure 4). In the study area, of 1243 km^2, approximately 11.5% are affected by flooding, which mainly includes areas near rural areas.

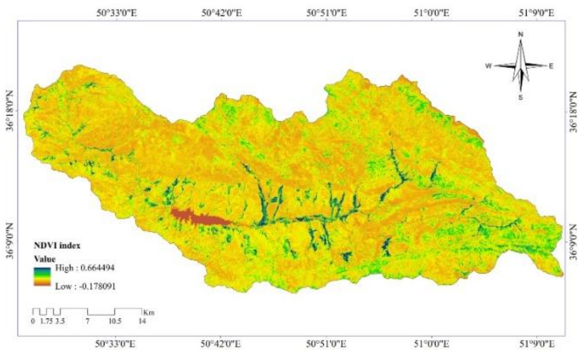

Figure 4. Normalized difference vegetation index of the Taleghan watershed

Since that the purpose of the LC index is to obtain separate areas with only tree and shrub cover and pasture, so by using the CON command in the Arcmap, the NDVI index was divided into two classes with cover and without cover (Figure 5).

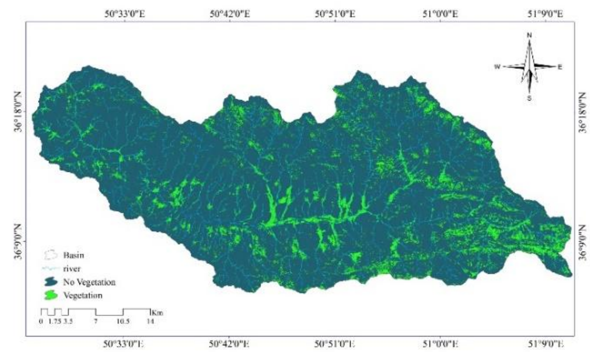

Figure 5. Classification of vegetation map in the studied watershed

Consequently, two methods were used to extract the relevant maps to determine the flood effects of each land use. In the first method, the significance of each factor was derived in relation to the correlation coefficient and the P-value statistic (Table 1). Table 1 shows that coverage was significantly and inversely associated with flooding in the study area, whereas urban areas were positively and significantly associated with flooding.

Table 1. A study of the impact of land use on flooding based on Spearman's correlation coefficient

		flood	bare soil	crop	forest	urban	NDVI
flood	Correlation Coefficient	1.000	0.75 **	-0.59**	-0.62*	.066**	-0.45*
	Sig. (2-tailed)	.	.006	.001	.06	.000	.009

**.The correlation is significant at the 0.01 level (2-tailed).
*. The correlation is significant at the 0.05 level (2-tailed).

The second method used ArcMap's overlay command to pair two boards at once (Figure 6). According to Figure 6, the flood zones were mainly restricted to areas outside of the land where there was LC and trees.

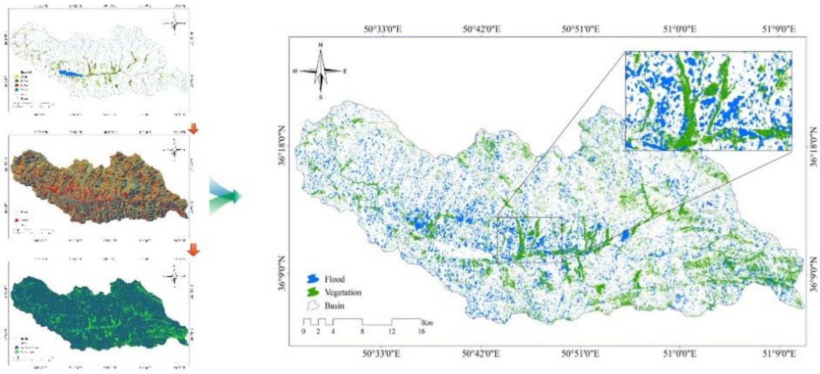

Figure 6. Homogeneous areas in flooding

4- Discussion and conclusion

Many factors must be considered flood zoning, and each has a different degree of importance. But because of the limitations that exist in preparing some layers and the limitations that exist because of the long process of the method. The use of multiple layers of information causes excessive model complexity, cost and time-consuming analysis and treatment of the method. Thus, simplifying models to extract effective parameters may help to determine flood factors. In this study, because of the mountainous nature of the Taleghan watershed, flood impacts were limited to two categories: LU and LC. Flood, land use and vegetation maps for the case study were extracted using 1-2 Sentinel images with a spatial resolution of 10 m. Flood maps were extracted based on pre- and post-flood changes in the study area. Within the study area, most of the urban, agricultural and forest land is confined around the river (Figure 2). But the flooding began upstream of the rural areas (Figure 3), which shows that there was a factor other than LU changes. Because of the limited agricultural land and gardens due to the mountainous nature of the region, most residents of the Taleghan region are involved in livestock farming. The high number of livestock in this area, as well as the presence of annual vegetation and semi-dense grasslands, have caused the land surface to be devoid of protective cover for most of the year. This may be one of the main factors contributing to flooding in this area. A map of the NDVI index with a spatial resolution of 10 m was prepared to demonstrate the role of coverage in flood control (Figure 4). There was virtually no flooding of areas where there was vegetation (Soltani et al., 2021; Bevington et al., 2022). In examining the role of land use change, it was noted that flooding has occurred in urban areas. Because residential uses and gardens have been created in streams that are the scene of the flood, and as a result, flood exposure has increased in those area (Castells-Quintana et al., 2022). As such, the use of simple modelling and zoning of flood-prone areas can help manage more flood-prone areas. In the studied area, in addition to the mentioned factors of slope and height and other photographic and climate parameters, it has also been effective on floods in this area, which should be considered in the studies.

REFERENCES

1. Bevington, A. E., Twilley, R. R., Sasser, C. E., 2022. Deltaic floodplain wetland vegetation dynamics along the sediment surface elevation gradient and in response to disturbance from river flooding and hurricanes in Wax Lake Delta, Louisiana, USA. *Geomorphol*, 398, 108011.
2. Braun, M., Herold. M., 2004. February: Mapping imperviousness using NDVI and linear spectral unmixing of ASTER data in the Cologne-Bonn region (Germany). In remote sensing for environmental monitoring, *Gis Applications, and Geology iii* (Vol. 5239, pp. 274-284). SPIE.
3. Talbot, C. J., Bennett, E. M., Cassell, K., Hanes, D. M., Minor, E. C., Paerl, H., Peter A., Vargas, R.R., Vidon, P.G., Wollheim, W., Xenopoulos, M. A., 2018. The impact of flooding on aquatic ecosystem services. *Biogeochemistry*, 141(3), 439-461.
4. Carvalho, V. S., da Cunha, Z. A., Alvarenga, L. A., Beskow, S., de Mello, C. R., Martins, M. A., de Oliveira, C. D. M., 2022. Assessment of land use changes in the Verde River basin using two hydrological models. *J. South Am. Earth Sci*, 103954.
5. Castells-Quintana, D., del Pilar Lopez-Uribe, M., McDermott, T. K., 2022. Population displacement and urban conflict: Global evidence from more than 3300 flood events. *J. Develop. Econ*, 158, 102922.

6. Gitelson, A. A., Merzlyak, M. N., 1998. Remote sensing of chlorophyll concentration in higher plant leaves. *Adv. Space Res*, 22(5), 689-692.
7. Kulkarni, K., Vijaya, P. A., 2021. NDBI Based Prediction of Land Use Land Cover Change. *J. India. Soc. Remote Sens*, 49(10), 2523-2537.
8. Li, J., Bortolot, Z. J., 2022. Quantifying the impacts of land cover change on catchment-scale urban flooding by classifying aerial images. *J. Cleaner Prod*, 344, 130992.
9. Liang, Y. Song, W., 2022. Integrating potential ecosystem services losses into ecological risk assessment of land use changes: A case study on the Qinghai-Tibet Plateau. *J. Environ. Manage*, 318: 115607.
10. Khadka, M., Kayastha, R. B., Kayastha, R., 2020. Future projection of cryospheric and hydrologic regimes in Koshi River basin, Central Himalaya, using coupled glacier dynamics and glacio-hydrological models. *J. Glaciol*, 66(259), 831-845.
11. Pal, S. C., Chowdhuri, I., Das, B., Chakrabortty, R., Roy, P., Saha, A., Shit, M., 2022. Threats of climate change and land use patterns enhance the susceptibility of future floods in India. *J. Environ. Manage*, 305, 114317.
12. Parven, A., Pal, I., Witayangkurn, A., Pramanik, M., Nagai, M., Miyazaki, H., Wuthisakkaroon, C., 2022. Impacts of disaster and land-use change on food security and adaptation: Evidence from the delta community in Bangladesh. Int. *J. Disaster Risk Reduct*, 78, 103119.
13. Purswani, E., Verma, S., Jayakumar, S., Khan, M. L., Pathak, B., 2022. Examining and predicting land use change dynamics in Gandhinagar district, Gujarat, India. *J. Urban Manag*, 11(1), 82-96.
14. Rahman, M. Ningsheng, Ch. Mahmud, G.I. slam, M.M. Pourghasemi, H.R. Ahmad, H. Habumugisha, J.M. Muhammad, R., Washakh, A., Alam, M., Liu, E., Han, Zh., Ni, H., Shufeng, T., Dewan, A., 2021. Flooding and its relationship with land cover change, population growth, and road density. *Geosci. Front*, 12 (6): 101224.
15. Rigby, A.M.F., Butcher, P., W.S.Ritsos, P.D., Patil, S. D., 2022. LUCST: A novel toolkit for Land Use Land Cover change assessment in SWAT+ to support flood management decisions. *Environ. Modell. & Software*, 105469.
16. Soltani, K., Ebtehaj, I., Amiri, A., Azari, A., Gharabaghi, B. Bonakdari, H., 2021. Mapping the spatial and temporal variability of flood susceptibility using remotely sensed normalized difference vegetation index and the forecasted changes in the future. *Sci. Total Environ*, 770, p.145288.
17. Tilahun, A. K., 2015. Land use land cover change and its implication on surface runoff: a case study of Baro River basin in south western Ethiopia. *J. Environ. Earth Sci*, 5(8).
18. Tsai, Y.H., Stow, D., Chen, H.L., Lewison, R., An, L., Shi, L., 2018: Mapping vegetation and land use types in Fanjingshan National Nature Reserve using google earth engine. Remote Sens, 10(6), 927.
19. Wahlstrom, M., Guha-Sapir, D., 2015. The Human Cost of Weather-related Disasters 1995–2015. UNISDR, Geneva, Switzerland (2015).
20. Wang, Y., Li, Z., Tang, Z., Zeng, G., 2011. A GIS-based spatial multi-criteria approach for flood risk assessment in the Dongting Lake Region, Hunan, Central China. *Water Resour. Manage*, 25 (13): 3465-3484.
21. Xu, Y., Yu, L., Zhao, F.R., Cai, X., Zhao, J., Lu, H., Gong, P., 2018. Tracking annual cropland changes from 1984 to 2016 using time-series Landsat images with a change-detection and post-classification approach: Experiments from three sites in Africa. *Remote Sens. Environ*, 218, 13-31.